An investigation of ionizing radiation damage in different SiGe processes*

Pei Li(李培)[1], Mo-Han Liu(刘默寒)[3], Chao-Hui He(贺朝会)[1,†], Hong-Xia Guo(郭红霞)[2], Jin-Xin Zhang(张晋新)[1], and Ting Ma(马婷)[1]

[1] School of Energy and Power Engineering, Xi'an Jiaotong University, Xi'an 710049, China
[2] Northwest Institution of Nuclear Technology, Xi'an 710024, China
[3] Key Laboratory of Functional Materials and Devices for Special Environments of Chinese Academy of Sciences, Xinjiang Technical Institute of Physics & Chemistry, Chinese Academy of Sciences, Urumqi 830011, China

(Received 28 February 2017; revised manuscript received 27 April 2017; published online 20 June 2017)

Different SiGe processes and device designs are the critical influences of ionizing radiation damage. Based on the different ionizing radiation damage in SiGe HBTs fabricated by Huajie and an IBM SiGe process, quantitatively numerical simulation of ionizing radiation damage was carried out to explicate the distribution of radiation-induced charges buildup in KT9041 and IBM SiGe HBTs. The sensitive areas of the EB-spacer and isolation oxide of KT9041 are much larger than those of the IBM SiGe HBT, and the distribution of charge buildup in KT9041 is several orders of magnitude greater than that of the IBM SiGe HBT. The result suggests that the simulations are consistent with the experiment, and indicates that the geometry of the EB-spacer, the area of the Si/SiO_2 interface and the isolation structure could be contributing to the different ionizing radiation damage.

Keywords: different silicon–germanium process, ionizing radiation damage, numerical simulation

PACS: 85.30.Pq, 61.80.Az, 73.40.Lq, 61.80.–X **DOI:** 10.1088/1674-1056/26/8/088503

1. Introduction

Silicon–germanium heterojunction bipolar transistors (SiGe HBTs) have been extensively tested for ionizing radiation hardness assurance for space applications in the numerous publications. It is well established that SiGe HBTs have a very favorable built-in ionizing radiation (TID and ELDRS) tolerance to multi-Mrad levels by process regardless of dose rate.[1–3] The SiGe HBTs under test used in these key references for ionizing radiation effects are all manufactured by the IBM SiGe process. Several generations of these SiGe HBTs related to ionizing radiation research also show that ionizing radiation effects are found to be nearly nonexistent.[4–6] However, different SiGe processes may involve different HBT structures and device designs that are the critical influences of ionizing radiation damage. In our work, ^{60}Co γ-ray irradiation experiments were performed to investigate the ionizing radiation damage for SiGe HBTs manufactured by Huajie-tech.[7,8] These SiGe HBTs named by KT1151 and KT9041 are investigated under dose rates of 80 rad(SiO_2)/s and 0.13 rad(SiO_2)/s with a ^{60}Co γ-ray irradiation source. The results of the experiments show that the radiation damage is different after prolonged annealing. The result shows a time-dependent effect for the KT1151, while for the KT9041, it seems that the degradations of low dose rate irradiation are higher than those of the high dose rate, demonstrating that there is an ELDRS.[9]

To date, no studies on ionizing radiation damage for different SiGe processes have been reported. However, the nature of radiation-induced oxide charge and annealing in Si/SiO_2 is not easily characterized via electrical measurements. TCAD simulations were commonly used to explain the radiation problems that traps must be located uniformly throughout the device, and additional interface traps must be located around the emitter-base spacer (EB-spacer) oxide edge. Most of the radiation-induced recombination occurs inside the EB-space charge region, leading to the G/R center dominated recombination decreases, giving a reduction in base current. The magnitude of the leakage decrease depends on the quasi-Fermi levels and hence the EB bias conditions. As confirmed with simulation, this proposed mechanism can indeed give rise to a decrease in base current, consistent with the experimental observations. At the same time, radiation-induced traps are generated in the device, which ultimately halts the I_B decrease and causes an increase in I_B.[10,11] Three-dimensional (3D) numerical simulations of ionizing radiation effects are carried out to explicate the distribution of radiation-induced charges buildup in KT9041 and IBM SiGe HBTs. The result suggests that the geometry of emitter and base, thickness of oxide, area of Si/SiO_2 interface, and isolation structure could be contributed to different ionizing radiation responses in KT9041 and IBM SiGe HBTs.

*Project supported by the National Natural Science Foundation of China (Grant Nos. 61274106 and 61574171).
†Corresponding author. E-mail: hechaohui@mail.xjtu.edu.cn
© 2017 Chinese Physical Society and IOP Publishing Ltd

2. Ionizing radiation damage in different process SiGe HBTs

The ^{60}Co γ-ray irradiation was performed for KT1151 and KT9041 SiGe HBTs with a water-well ^{60}Co γ-ray source at the Xinjiang Technical Institute of Physics & Chemistry of Chinese Academy of Sciences. The high dose rate (HDR) and low dose rate (LDR) were conducted at dose rates of 80 rad(SiO_2)/s and 0.13 rad(SiO_2)/s, respectively. The room temperature annealing for high dose rate irradiation was performed and the annealing time was the same as the duration time of the low dose rate irradiation. All samples are irradiated to accumulated dose levels of 50, 100, 200, 300, 500, 800, and 1000 krad(SiO_2). A Pb/Al box was adopted to decrease the flux of the secondary γ ray and ensure a monochromatic ^{60}Co γ-ray spectrum. The devices under test were mounted on the irradiation boards with an all-grounded bias ($V_B = V_E = V_C = 0.0$ V) during the irradiation and annealing processes. The electrical tests of the transistor were made on a KETHLEY4200 semiconductor parameter analyzer. In order to compare the degradation of different process SiGe HBTs quantitatively, a parameter of excess base leakage current ($\Delta I_B = I_{Bpost} - I_{Bpre}$) is introduced. The voltage $V_{BE} = 0.7$ V is chosen to look at the excess base current as illustrated in Fig. 1.

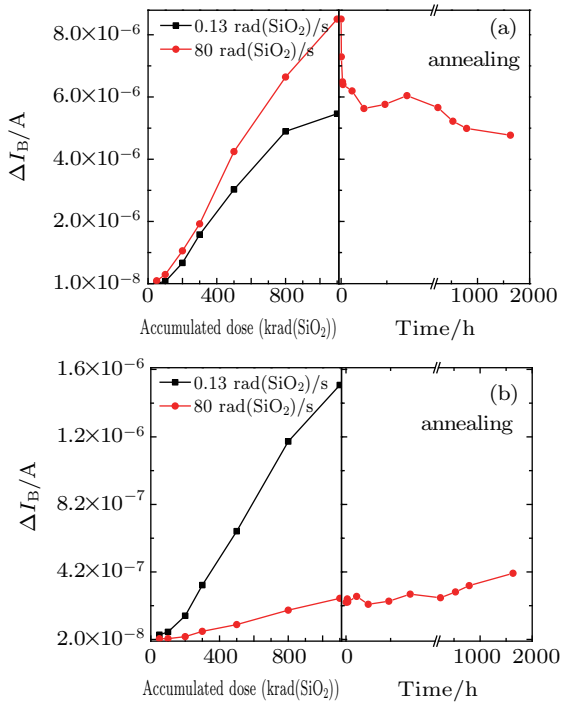


Fig. 1. (color online) Excess base current as a function of accumulated total dose and annealing time at V_{BE} of 0.6 V. (a) KT1151 SiGe HBT; (b) KT9041 SiGe HBT.

It is indicated that the base leakage current increases with accumulated total dose for both low and high dose rates irradiations, but there is a great deal of difference between the KT9041 and KT1151 SiGe HBTs. The ΔI_B of the KT1151 for the high dose rate is greater than that of the low dose rate and decreased dramatically in the first few tens of hours of annealing, recovering quickly to the value of the irradiation at 1100 krad(SiO_2) under the low dose rate, and then remains unchanged, which shows there is a TDE. For the KT9041, the ΔI_B for high dose rate irradiation cannot rebound to the level of low dose rate irradiation even after a long-term annealing, i.e., a "true" dose rate effect exists in KT9041SiGe HBTs.

3. 3D TCAD simulation

3.1. Device descriptions

In order to explain the mechanisms of different ionizing radiation damage in Huajie and IBM SiGe HBTs, numerical simulations were performed respectively. Figure 2(a) is the two-dimensional (2D) cross section of SiGe HBTs manufactured by Huajie-tech named KT9041, and its basic structure is similar to the bulk silicon vertical NPN bipolar transistor. The collector contact is routed through a heavily doped n^+ buried layer and the p^+ epitaxial base is grown above the local oxidation of silicon (LOCOS). The doping concentration of intrinsic base is about 1×10^{19} cm^{-3}, and the content of Ge gradually changes from 0% to 20% at the

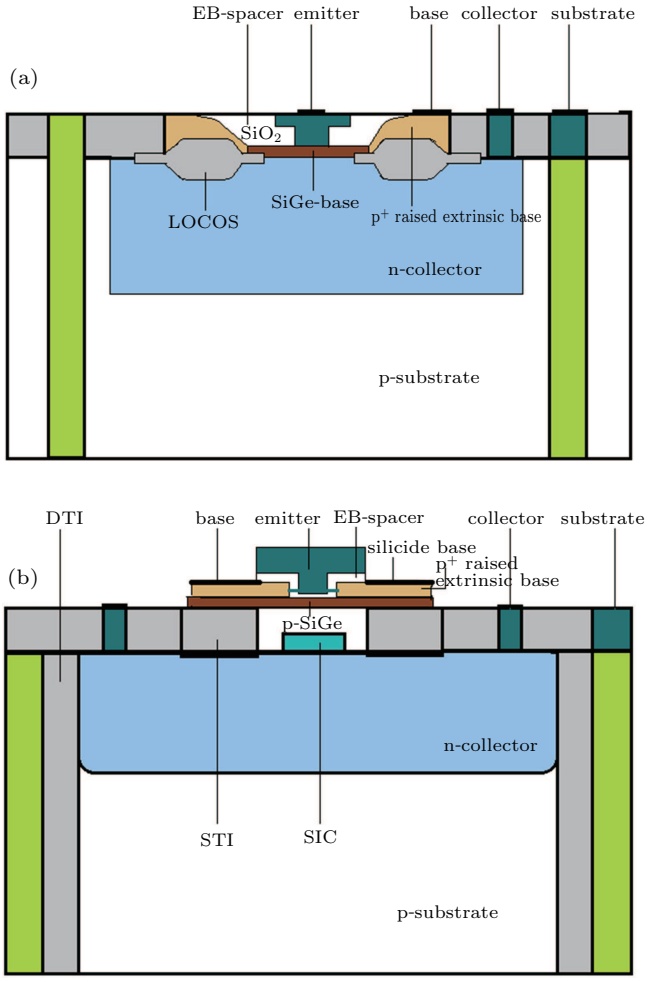


Fig. 2. (color online) Schematic diagram of device cross section of the SiGe HBTs. (a) KT9041, (b) IBM 8HP (not to scale).

emitter/base and base/collector junctions. The doping concentration of the emitter is 1.5×10^{20} cm^{-3} and the area of each emitter finger is 0.4 μm×20 μm. A ring wall of heavily doped boron leads out of the substrate contact near the edge of the device, and the emitter and substrate are connected together via a metal inter-connection.[12] Figure 2(b) shows the 2D cross section of IBM SiGe HBTs fabricated by IBM'8HP technology; the process starts with the formation of a heavily arsenic-doped sub-collector buried layer formed by ion implantation, on top of which a lightly doped epitaxial layer is grown that serves as the collector region. Shallow trench isolation (STI) without the use of mesa etching generally employed in SiGe HBTs, leads to a planar topography and dense layout.[13]

3.2. Device modeling

According to the process and layout information of the device described in Section 2, a Sentaurus Structure Editor and Sentaurus Device from the Sentaurus TCAD simulator of Synopsys were used for building the 3D models. The physical models considered for these devices include Phillips unified mobility, SRH recombination, Auger recombination, velocity saturation, and bandgap narrowing (BGN). A two-stage degradation model was implemented in numerical simulations and the creation of oxide-trapped charges and interface states proceeded via a two stage process. The 3D models of KT9041 and IBM 8HP SiGe HBTs generated from the Sentaurus Structure Editor are shown in Figs. 3(a) and 3(b), respectively. The test data of 8HP SiGe HBT used in this calibration originate from the reference.[14] The current gain is the most outstanding electrical property in SiGe HBTs. Thus, the Gummel curve which was obtained by simulation is compared with the curves measured by a KEITHLEY 4200 until a reasonable model is built, as seen from Fig. 4.

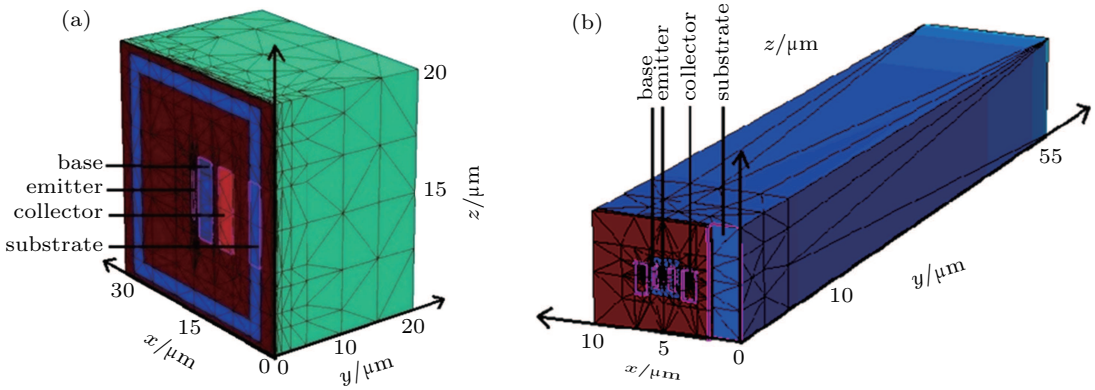


Fig. 3. (color online) 3D models of SiGe HBT. (a) KT9041; (b) IBM 8HP.

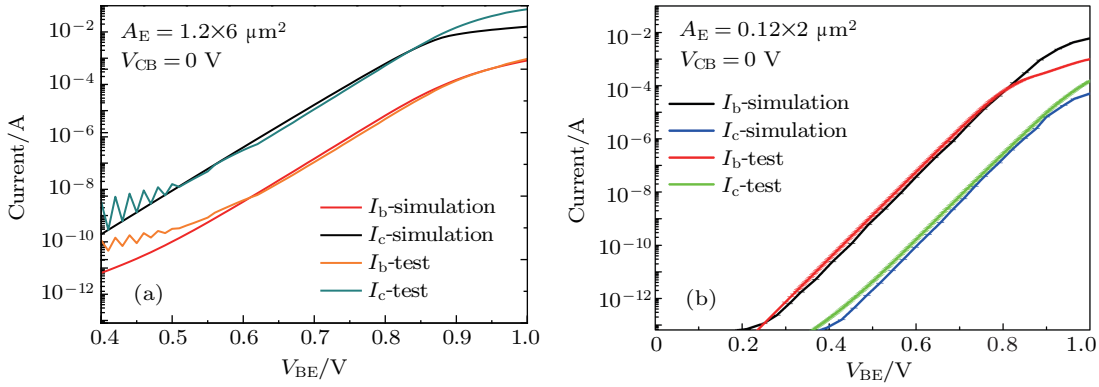


Fig. 4. (color online) Calibration of Gummel characteristic for SiGe HBTs. (a) KT9041; (b) IBM 8HP.

3.3. Numerical simulations

The mechanisms governing ionizing radiation damage can be described by space charge effects, carrier recombination and trapping, and proton release. In the two-stage degradation model, the oxygen vacancy (state 1) is a neutral Si–Si weak bond which features an electron level far below the silicon valence band edge. This neutral defect can capture a hole and cause the break of the weak bond, resulting in structural relaxation. During this process, one of the silicon atoms takes the positive charge, and the other silicon atom carries a dangling bond with an energy level close to the silicon band gap. Since E' centers (state 2) are capable of trapping or detrapping charge carriers from the silicon substrate and the repeated exchange of charge carriers is reflected in transferring back and forth between state 2 and state 3. The neutral charge state (state 3) may return back to a neutral Si–Si

bond by surmounting a thermal barrier. Mentioned above is the first stage of the two-stage degradation model. During the second stage, unpassivated Si–H bonds are triggered by a reaction with hydrogen and the increased holes concentration enhances the creation of fixed positive charge with a P_b center (state 4). In the two-stage degradation model, the involved energy levels and activation energies are distributed widely and treated as random variables. The trap level of the oxygen vacancy, E' center and P_b centers are -1.14 eV$\sim$ 0.31 eV, 0.01 eV$\sim$ 0.3 eV, and 0.01 eV$\sim$ 0.5 eV respectively by default. Holes are the dominant carrier in the oxide bulk due to their low intrinsic mobility in SiO_2, compared to the intrinsic mobility of electrons. The electron and hole capture cross sections are $\sigma_n = 1.08 \times 10^{-15}$ cm^2 and $\sigma_p = 1.24 \times 10^{-14}$ cm^2 respectively. Numerical simulation is started by the addition of oxygen vacancy at sensitive Si/SiO_2 interfaces. A random sampling technique is used to obtain the average change of the interface charges.[15,16] In order to investigate the impact of EB-spacer geometry and isolation oxide structure on ionizing radiation effect in different SiGe processes, the two-stage degradation model is implemented in 3D models and numerical simulations are performed on KT9041 and IBM SiGe HBTs.

4. Discussion

Ionizing radiation damage of a bipolar device is mainly caused by an increasing surface recombination velocity due to the buildup of radiation-induced charge at the sensitive Si/SiO_2 interface. Previous studies have shown that the damage of ionizing radiation in SiGe HBTs is driven predominately by two sensitive areas: 1) the Si/SiO_2 interface underneath the dielectric "spacer" separating the emitter and base regions (EB-spacer). The buildup of radiation-reduced charges over the EB-spacer will deplete the lowly doped base region and the total depleted surface area in SiGe HBTs increases. 2) Si/SiO_2 interface at the edge of STI or LOCOS isolation oxide. Radiation-induced charge buildup in LOCOS or STI normally dominates the radiation-induced degradation of ICs and induces large leakage currents. For the KT9041 with LOCOS isolation, the beak region originally has more defects due to the stress by manufacture. For a better view, 2D cross sections of KT9041 and IBM 8HP SiGe HBT models are depicted in Fig. 5.

Different SiGe processes may involve different HBT structures and device designs that are the critical influence of ionizing radiation damage. Seen from Fig. 5(a), the LOCOS oxide is produced by a local reaction of silicon and water at high temperature. The epitaxial base region of KT9041 SiGe HBT is grown above the LOCOS oxide that increases the area of the sensitive Si/SiO_2 interface. At the edge of the LOCOS isolation, the oxide thickness decreases and this transition region is referred to as the "bird's beak" region. The beak region originally has more defects due to the stress by manufacture and the beak region is so thin that the electric fields will effectively impact the induced charges in this area. Some researchers also explain that the ΔI_B growth is induced by the non-ideal factors of currents that comprise the recombination current of the depletion region and the surface recombination current. On one side, the surface of the p-type base region depletes because the E' centers in the oxide layers forms additional electric fields near pn-junctions. In this case, the volume of the depletion layer increases so that the base recombination current rises. On the other side, P_b centers play a role in recombination at the $Si–SiO_2$ interface; thus, the surface recombination current rises.

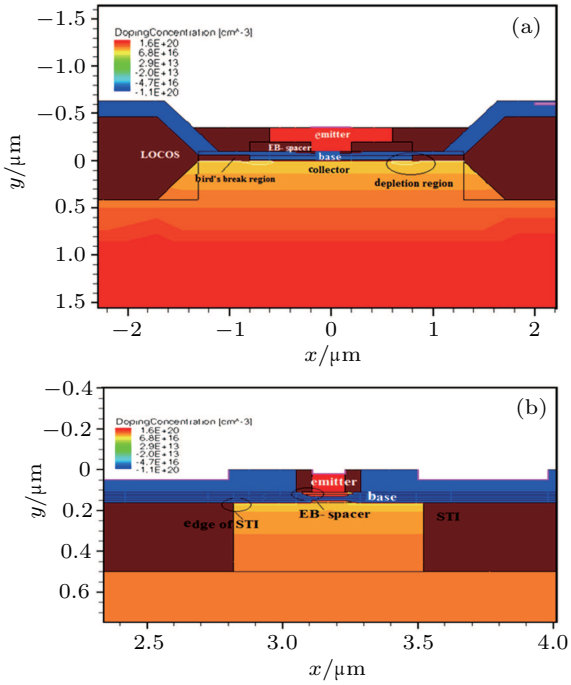


Fig. 5. (color online) Cross-section of 3D SiGe HBT models. (a) KT9041; (b) IBM 8HP.

Figure 5(b) shows that the charges buildup in the LOCOS oxide of KT9041 SiGe HBT turn on a parasitic leakage path, but the STI process does not involve the growth of an isolation region. More importantly, the epitaxial base of IBM 8HP SiGe HBT located immediately below the EB-spacer oxide region, effectively confining the radiation-reduced damage and its effect on the emitter-base junction. In order to investigate the impact of EB-spacer geometry and isolation oxide structure on ionizing radiation damage in different process SiGe HBTs, the two-stage degradation model is implemented in 3D models and numerical simulations are performed on KT9041 and IBM 8HP SiGe HBTs. As we know, the quality of the oxide, in terms of defect density, is process-dependent. The oxygen

vacancy is the dominant defect in SiO_2, and acts as deep-hole traps, capturing holes that remain localized very near the interface. To conduct quantitative analysis on the charge buildup in SiGe HBTs, the initial density of oxygen vacancy added to Si/SiO_2 interfaces are both $1.0 \times 10^{13}/cm^2$. However, the distribution of oxygen vacancies in KT9041 and IBM 8HP SiGe HBTs are very different in spite of the identical oxygen vacancy density.

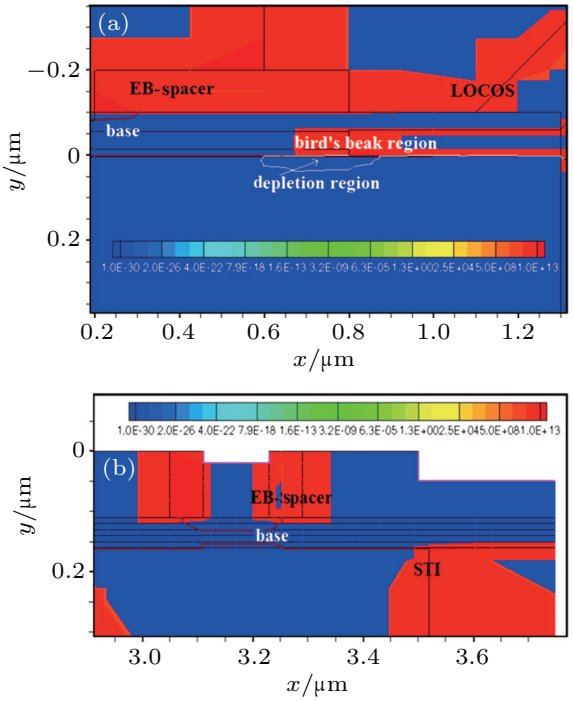


Fig. 6. (color online) Density of oxygen vacancy in SiGe HBT models at state 1. (a) KT9041; (b) IBM 8HP.

Seen from Fig. 6(a), oxygen vacancies are added to each Si/SiO_2 interface of KT9041 SiGe HBT, and the distribution is labeled at different locations. For Fig. 6(b), the oxygen vacancies are distributed in IBM 8HP SiGe HBT and mainly located at the EB-spacer and the edge of STI oxide.

During the irradiation, the electron–hole pairs generate owing to the energy deposition in the process of particles or photons passing through oxide. A fraction of the electron–hole pairs have recombined, and the electrons have been swept out of the oxide layer by the electric field in a picosecond. The remaining holes drift slowly toward the oxide layers through the "jump" mechanism. Some holes are trapped in the intrinsic defects at the Si/SiO_2 interface and captured subsequently by the oxygen vacancies, finally creating the positive oxide trap charges or E' centers.

Figure 7 shows the distribution of positive oxide trap charges for KT9041 and IBM 8HP SiGe HBT, respectively. For the case of KT9041 SiGe HBT, the positive oxide trap charges are mainly located in the EB-spacer, the bird's beak region and the edge of LOCOS oxide as well as the same rule with oxygen vacancies. In IBM 8HP SiGe HBT, the density of the positive oxide trap charges in EB-spacer and edge of STI oxide is one order of magnitude less than that of KT9041 SiGe HBT. E' centers generally located within a few nanometers of the Si/SiO_2 interface and can exchange charges via electron tunneling on time scales of microseconds to seconds.

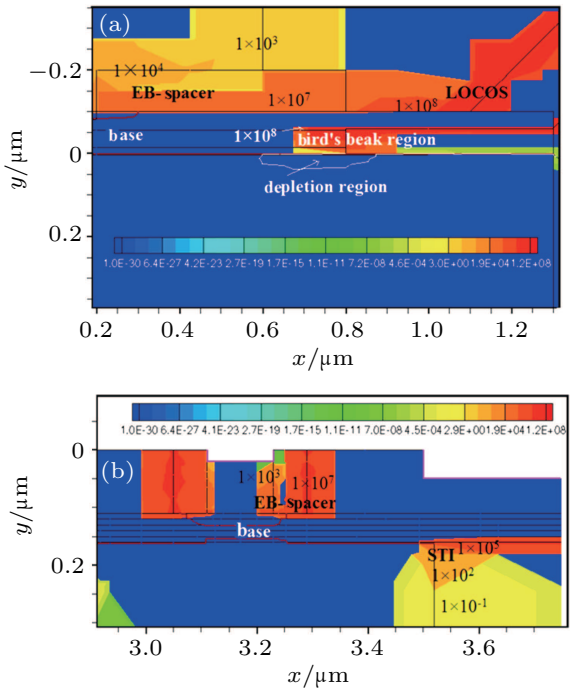


Fig. 7. (color online) Density of positive oxide trap charge in SiGe HBT models at state 2. (a) KT9041; (b) IBM 8HP.

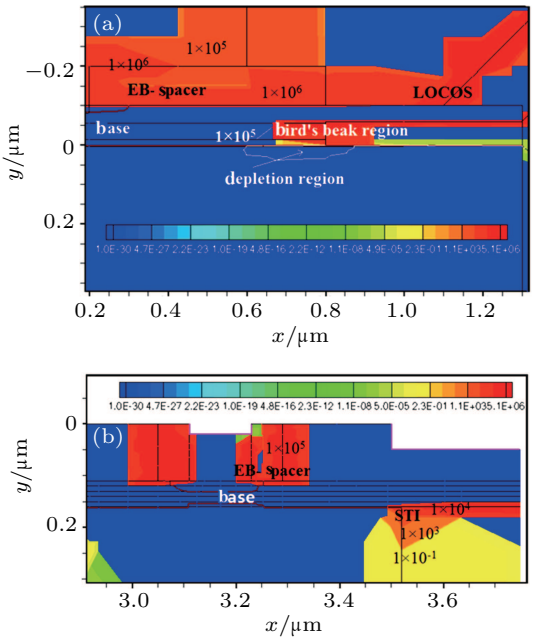


Fig. 8. (color online) Density of neutral center in SiGe HBT models at state 3. (a) KT9041; (b) IBM 8HP.

Therefore, the neutral centers were originated from positive oxide trap charges by emitting holes and the distribution of neutral centers have the same rule with positive charges as shown in Fig. 8. Unlike positive oxide traps, interface states

are located exactly at the interface. There is essentially no barrier to trapping and de-trapping of carriers at the Si/SiO_2 interface. The interface state can therefore have a significant effect on the carrier mobility and recombination rates of carriers at the sensitive interface. The creation of an interface state or P_b center primarily relies on the presence of H^+ near the interface. Protons diffusing or driven by the electric field to the Si/SiO_2 interface can remove hydrogen atoms from Si–H bonds. The second stage of the two-stage models is illustrated in Fig. 9. The distribution of interface states in KT9041 SiGe HBT is widely spread and the density is several orders of magnitude greater than that of IBM 8HP SiGe HBT, especially for the interface states buildup in the bird's beak region and the edge of LOCOS oxide. Consequently, radiation-induced charges buildup in KT9041 SiGe HBT along with the EB-spacer, bird's beak region and edge of LOCOS oxide are distributed more widely and densely than that of IBM 8HP SiGe HBT.

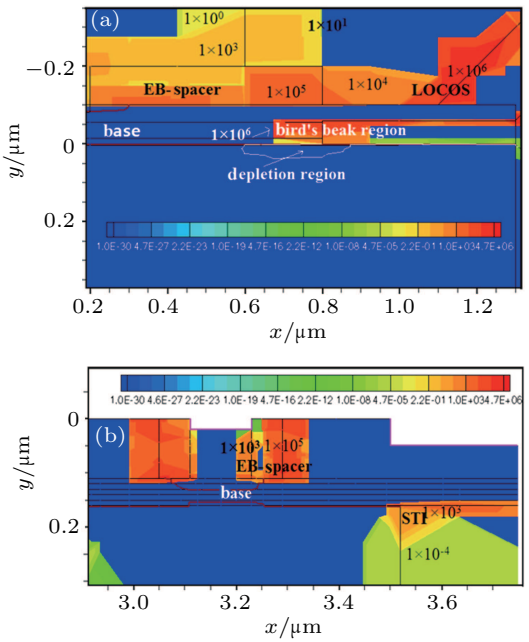


Fig. 9. (color online) Density of interface trap charge in SiGe HBT models at state 4: (a) KT9041; (b) IBM 8HP.

5. Conclusion

Different HBT structures and device designs contribute to the different ionizing radiation damage. In this work, quantitative simulations of the radiation-induced charge in the sensitive Si/SiO_2 interface were performed on the KT9041 and IBM SiGe HBTs. The different ionizing radiation damages in these two SiGe processes are driven predominately by the sensitive Si/SiO_2 interface in the EB-spacer and edge of the isolation oxide. It is well established that the simulation results are consistent with the experimental results. The areas of Si/SiO_2 interface in the EB-spacer and isolation oxide of KT9041 are much larger than those of IBM SiGe HBT, and the distribution of charge buildup in KT9041 is several orders of magnitude greater than that of the 8HP SiGe HBT, especially for the bird's beak region and edge of LOCOS oxide. The charges buildup in the LOCOS oxide of KT9041 turn on a parasitic leakage path while the STI process of IBM SiGe HBT does not involve the growth of an isolation region. More importantly, the epitaxial base of IBM SiGe HBT is located immediately below the EB-spacer oxide region, effectively confining the radiation-reduced damage. All these results suggest that the geometry of the EB-spacer, the area of the Si/SiO2 interface and the isolation structure could be contributing to the different ionizing radiation damage, revealing that different fabrication processes of SiGe HBTs will lead to different ionizing radiation damage.

References

[1] Cressler J D 2013 *IEEE Trans. Nucl. Sci.* **60** 3
[2] Hansen D L, Pong S, Rosenthal P and Gorelick J 2007 "Total Ionizing Dose Testing of SiGe 7HP Discrete Heterojunction Bipolar Transistors for ELDRS Effects", *Radiation Effects Data Workshop*, pp. 215–220
[3] Zhang J, Guo Q, Guo H and Lu W 2016 *Trans. Nucl. Sci.* **63** 2
[4] Fleetwood Z E, Cardoso A S, Song I and Wilcox E 2014 *IEEE Trans. Nucl. Sci.* **61** 6
[5] Banerjee G, Niu G, Cressler J D and Clark S D 1999 *IEEE Trans. Nucl. Sci.* **46** 6
[6] Haugerud B M, Pratapgarhwala M M, Comeau J P, Sutton A K, Prakash A P G, Cressler J D, Marshall P W, Marshall C J, Ladbury R L and El-Diwany M 2006 *Solid State Electron.* **50** 2
[7] Sun Y, Fu J, Xu J, Wang Y, Zhou W, Zhang W, Cui J, Li G and Liu Z 2014 *Nucl. Instrum. Methods Phys. Res.* **738** 2
[8] Liu M, Lu W, Ma W, Wang X, Guo Q, He C, Jiang K, Li X and Xun M 2015 *Chin. Phys. C* **40** 3
[9] Sun Y, Fu J, Xu J, Wang Y, Zhou W, Zhang W, Cui J, Li G and Liu Z 2014 *Physica B: Phys. Conden. Matter* **434** 2
[10] Sutton A K, Prakash A P G and Jun B and Zhao E 2006 *Trans. Nucl. Sci.* **53** 6
[11] Jiménezmolinos F, Gámiz F, Palma A, Cartujo P and Lópezvillanueva J A 2002 *J. Appl. Phys.* **91** 8
[12] Zhang J X, He C H, Guo H X, Tang D, Xiong C, Li P and Wang X 2015 *Microelectron. Reliab.* **55** 8
[13] Rieh J S, Jagannathan B, Greenberg D R, Meghelli M, Rylyakov A, Guarin F, Yang Z, Ahlgren D C, Freeman G and Cottrell P 2004 *IEEE Trans. Microwave Theor. Techniq.* **52** 10
[14] Yang H 2005 "3D Device Simulation of SEU-Induced Charge Collection in 200 GHz SiGe HBTs", Alabama: Auburn University
[15] Tsetseris L, Schrimpf R D, Fleetwood D M and Pease R L 2005 *IEEE Trans. Nucl. Sci.* **52** 6
[16] Sentaurus device user guide (version A-2008. 09). Synopsys, 2008